Coupling of PbS quantum dots to photonic crystal cavities at room temperature

Ilya Fushman,[a] Dirk Englund,[b] and Jelena Vučković[c]
Ginzton Laboratory, Stanford University, Stanford, California 94305

(Received 16 May 2005; accepted 6 October 2005; published online 5 December 2005)

We demonstrate the coupling of PbS quantum dot emission to photonic crystal cavities at room temperature. The cavities are defined in 33% Al, AlGaAs membranes on top of oxidized AlAs. Quantum dots were dissolved in poly(methylmethacrylate) and spun on top of the cavities. Quantum dot emission is shown to map out the structure resonances. This technique may prove to be viable sources for room temperature cavity coupled single photon generation for quantum information processing applications. Moreover, our results also indicate that such commercially available quantum dots can be used for passive structure characterization. The deposition technique is versatile and allows layers with different dot densities and emission wavelengths to be redeposited on the same chip. © *2005 American Institute of Physics*. [DOI: 10.1063/1.2138792]

Photonic crystal cavities are a very suitable medium for control and confinement of light on scales on the order of a cubic wavelength of light in the material. The small modal volumes and high quality factors for these cavities make them strong candidates for efficient single photon generation for quantum information processing,[1,2] low threshold lasing,[3] and nonlinear optics phenomena.[4] Our main motivation is the search for emitters that can be coupled to photonic crystal (PC) cavities in order to satisfy the constraints on indistinguishability and efficiency of the photon source for quantum information processing. Additional motivation is the characterization of the electromagnetic properties of passive elements to be used in photonic circuits. To date, successful generation of single photons coupled to PC microcavities has been demonstrated at cryogenic temperatures, because the emitters of choice degrade with an increase in temperature.[2] Room temperature generation of single photons has been observed from single molecules,[5] nitrogen vacancy centers,[6] and CdSe quantum dots,[7] but collection efficiencies were reduced due to lack of coupling to good cavities. These sources, with the exception of nitrogen vacancy centers, operate at visible wavelengths and are therefore difficult to combine with cavities made in high index semiconductor slabs. In contrast, PbS quantum dots (and other colloidal quantum dots such as PbSe) can be made to cover a very broad wavelength range. Furthermore, these dots can be easily deposited onto passive structures in a low index polymer and can be used to map out the resonances of the structures. This method is much easier than transmission and reflectivity type measurements on single cavities. Lastly, PbS quantum dots are successfully used as fluorescent labels in biological imaging applications. Cavity enhanced emission and collection efficiency from such dots could prove to be a valuable technique for targeted signal amplification of a target molecule bound to or in the vicinity of the resonant cavity.

Here, we report on the coupling of emission from PbS quantum dots to semiconductor photonic crystal cavities at room temperature. Photonic crystal cavities were made in a 160-nm-thick AlGaAs (33% Al) membrane on top of 500 nm of AlAs. The cavities were fabricated with standard electron beam lithography and dry etching methods. The Al rich substrate was then oxidized at 420 °C for 10 min in the presence of water vapor in order to create an index contrast of 3.4:1.6 between membrane and substrate. A scanning electron micrograph of the sample structure is shown in Fig. 1. PbS quantum dots emitting at 850 and 950 nm were obtained from Evident Technologies. The dots were dissolved together in 1% 75 K mW PMMA at a concentration of 0.1 mg/ml in toluene and spun onto the structures at 2 krpm, resulting in a 20–100 nm film (bulk spectra shown in Fig. 2). The coating was not uniform due to the small chip size $\sim(5\ \mathrm{mm})^2$ and presence of structures on the chip surface. This concentration of emitters corresponds to $\sim 10^2$ dots per-$\mu\mathrm{m}^2$ in a 100 nm membrane. The dots were kept under vacuum, and excited with femtosecond pulses from a Ti:saphire laser at 760 nm. Cavity spectra, collected under pulsed excitation, are shown in Fig. 3. The spectra reveal two orthogonally polarized modes as expected for this type of photonic crystal cavity. The linearly increasing background observed on the spectra can be explained by considering the emission profile of the dots and the reflectivity of the PMMA/AlGaAs/AlO_x structure, which leads to an almost linear emission profile of dots on the AlGaAs slab.

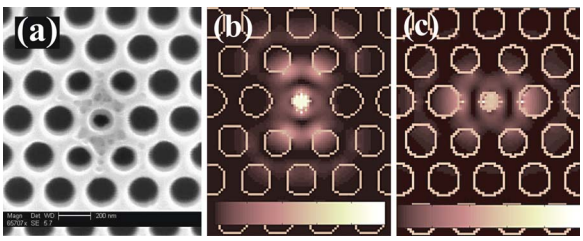

FIG. 1. (Color online) Left: Scanning electron micrograph showing the photonic crystal cavity (a). Middle: Simulated electric field intensity of the *x* (b) and *y* (c) dipole modes in the asymmetric cavity. The measured *Q* factors are ≈400 and 200, respectively.

[a]Also at: Department of Applied Physics, Stanford University, Stanford, CA 94305; electronic mail: ifushman@stanford.edu
[b]Also at: Department of Applied Physics, Stanford University, Stanford, CA 94305.
[c]Also at: Department of Electrical Engineering, Stanford University, Stanford, CA 94305.

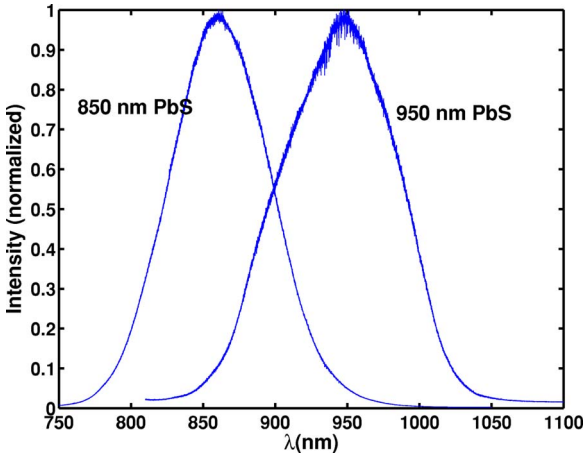

FIG. 2. (Color online) PbS quantum dot spectra: λ=850 and 950 nm dot spectra taken on a bulk silicon wafer.

The cavity used is shown in Fig. 1. The coupling between a cavity and emitter depends on both the spatial alignment and the orientation of the emitter dipole moment relative to the cavity field. The chosen cavities support two dipole type (electric field primarily polarized in x and y) cavity modes with maxima in the central hole in Fig. 1.[8] The asymmetric cavity was modeled using finite difference time domain (FDTD) methods.[1] The simulations predict the splitting between the two resonant peaks to be ≈43 nm, which is somewhat larger than the observed splitting of 37.5 nm and is likely due to deviations of fabricated structures from simulated ones. The quality factor (Q) is the figure of merit for these cavities, and can be written as

$$Q^{-1} = Q_{\parallel}^{-1} + Q_{\perp}^{-1}. \tag{1}$$

The earlier description separates the cavity losses into an out-of-plane loss which leads to directly observed emission, and losses into the Bragg mirrors in the plane of the two-dimensional crystal. The two components are calculated by measuring the energy loss through planes above and below the PhC slab ($Q_{\perp}$), and through the sides between the planes ($Q_{\parallel}$) in the FDTD simulation. The cavities investigated here have experimentally observed x-dipole Q's≈400 and y-dipole Q's≈200. These measurements correspond to the total Q given in 1, which is determined by the lowest of $Q_{\parallel}$ and $Q_{\perp}$. Simulations for the asymmetric cavity predict that the out of plane $Q_{\perp}\approx 8000$ for the x-dipole mode and ≈4000 for the y dipole. The simulated in-plane $Q_{\parallel}$ was only ≈450 and 400 for these modes, and thus limits the total Q. Q is unaffected in this case by the etch depth into the AlO_x substrate and the hole profile inside the substrate,[9] since the structure is backfilled with PMMA, whose refractive index is approximately that of AlO_x.[8] The two cavity modes are shown in Fig. 1(b). In a perfectly symmetric cavity, where the two holes above and below the defect are unperturbed, the x and y modes are degenerate and have a Q of ≈400. We shift the four holes in order to increase the Q factor for the x-dipole mode, as has been discussed in Refs. 1 and 8.

The photonic crystal can both enhance and reduce spontaneous emission (SE) rates for the quantum dots. The enhancement is desirable for photon generation and spectroscopy applications due to increased signal rate and strength. The figure of merit for this modification is the Purcell factor $F=\Gamma_C/\Gamma_0$. Here Γ is the emission rate in the cavity and Γ_0 is that without the cavity. The observed spontaneous emission rate for an emitter with dipole moment $\boldsymbol{\mu}$ at a point on the cavity can be derived from Fermi's Golden rule,[10] and the total rate takes the form

$$\frac{\Gamma_C}{\Gamma_0} = F_C\left(\frac{\mathbf{E}\cdot\boldsymbol{\mu}}{|\max\{\mathbf{E}\}||\boldsymbol{\mu}|}\right)^2 \frac{\Delta\lambda_c^2}{\Delta\lambda_c^2 + 4(\lambda-\lambda_c)^2} + F_{\mathrm{PC}}. \tag{2}$$

Here $\mathbf{E}$ is the electric field at the position of the emitter, V_{mode} is the cavity mode volume, and $\Delta\lambda$ is the detuning from the cavity resonance wavelength λ_c. For an emitter that is on resonance with the cavity and has a dipole moment aligned with the field, $F_C=(3\lambda_c^3 Q/4\pi^2 n^3 V_{\mathrm{mode}})$. The mode volume is calculated from the FDTD simulation results as $V_{\mathrm{mode}}=\int \epsilon|\mathbf{E}|^2/\max\{\epsilon|\mathbf{E}|^2\}d^3\mathbf{r}$, with ϵ as the position dependent dielectric constant. For this cavity, the volume has a value of $V_{\mathrm{mode}}=0.96(\lambda_c^3/n^3)$, where n is the index in AlGaAs. The term F_{PC} describes the modification of the SE rate due to the presence of the photonic crystal lattice and modes other than the cavity mode. This modification results in a suppression of the spontaneous emission.[2,11] The cavity mode volume can be quite accurately derived from FDTD calculations, and with the cavity Q derived from the spectra, we calculate $F_C\approx 30$. We can also derive an average value of the suppression F_{PC} from the experimental data. The total intensity collected by the spectrometer I_ϕ is given by the emission

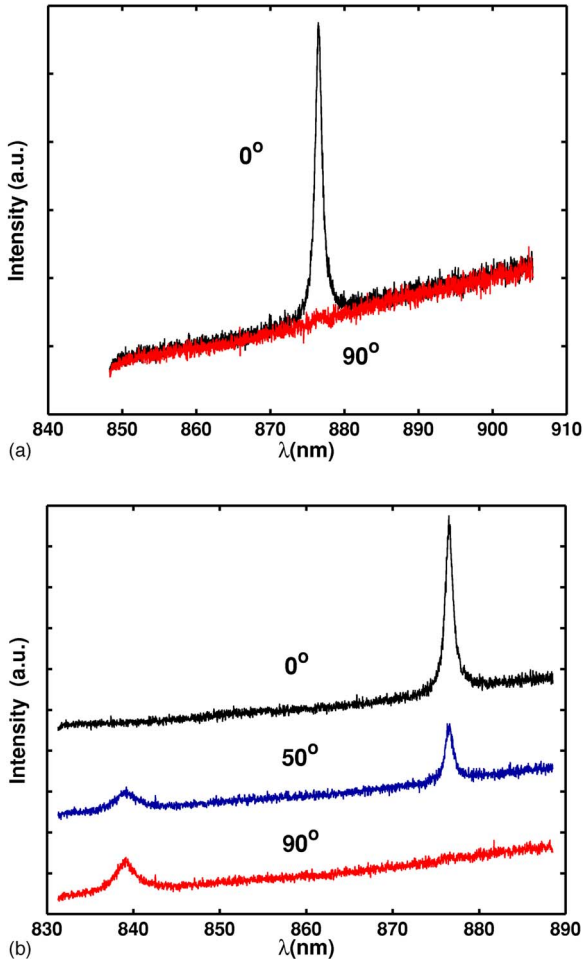

FIG. 3. (Color online) Cavity resonances mapped out by quantum dots in PMMA. Top: Polarization dependence of modes confirming that they are x and y dipole modes. Bottom: Ex dipole mode measured at two orthogonal polarizations. Angles refer to analyzer positions.

rate 2, integrated over the spatial and spectral density of the emitters

$$I_\phi = \Gamma_0 \int\int\int d\boldsymbol{\mu} d\lambda d^3\mathbf{r} \left\{ \eta_C F_C \cos(\phi) \left(\frac{\mathbf{E}\cdot\boldsymbol{\mu}}{|\max\{\mathbf{E}\}||\boldsymbol{\mu}|} \right)^2 \times \frac{\Delta\lambda_c^2}{\Delta\lambda_c^2 + 4(\lambda-\lambda_c)^2} + \eta_0 F_{PC} \right\} \rho(\lambda,\mathbf{r},\boldsymbol{\mu}). \quad (3)$$

Here ϕ is the value of the polarizer angle, η_C is the collection efficiency due to the cavity radiation profile, η_0 is the collection efficiency from an emitter embedded in the PMMA layer and uncoupled to the cavity, and $\rho(\lambda,\mathbf{r},\boldsymbol{\mu})$ contains the spectral and spatial distribution of the dots and the orientations of their dipole moments. The value of η_C can be estimated from numerically integrating the PC emission profile over the numerical aperture (NA) of the lens, and is $\eta_C \approx 8\%$. The coupling efficiency of the bulk emitter is given by the integral over the subcritical solid angle defined by the NA of the objective lens $\eta_0 = 1/4\pi \int_0^{2\pi} d\phi \int_0^{\arcsin(\mathrm{NA}/n_{\mathrm{PMMA}})} \sin(\theta) d\theta \approx 3\%$. (Here NA=0.5 and $n_{\mathrm{PMMA}}=1.5$.) Since the cavity modes are primarily linearly polarized, the ratio of the integrated intensities for polarizer angles of 0° and 90° gives

$$R = \frac{I_{0^\circ}}{I_{90^\circ}} \approx F_C \frac{\eta_C}{\eta_0} \left[\int\int\int d\boldsymbol{\mu} d\lambda\, d^3\mathbf{r} \rho(\lambda,\mathbf{r},\boldsymbol{\mu}) \left(\frac{\mathbf{E}\cdot\boldsymbol{\mu}}{|\max\{\mathbf{E}\}||\boldsymbol{\mu}|} \right)^2 \frac{\Delta\lambda_c^2}{\Delta\lambda_c^2 + 4(\lambda-\lambda_c)^2} \right] \Big/ \left[\int\int\int d\boldsymbol{\mu} d\lambda\, d^3\mathbf{r} F_{PC} \rho(\lambda,\mathbf{r},\boldsymbol{\mu}) \right] + 1. \quad (4)$$

Using the value of F_C and the x-dipole field, the average value of F_{PC} over the lattice around the cavity can thus be estimated from the spectra. Assuming random dipole orientation, the integral over $\boldsymbol{\mu}$ gives $\frac{1}{3}$. We take the spectral distribution of the dots to be Gaussian and centered at 850 and 950 nm with a full width at half maximum (FWHM) of 100 nm. The cavity lineshape is Lorentzian with a FWHM of 2 nm. The spatial density corresponds to the excitation of a uniform dot distribution by a Gaussian pulse with a FWHM of 600 nm in the x,y plane and uniform in z, since the layer is thin relative to the focal depth. The integral over the field is done numerically with the simulated cavity field components. The spectral data shown in Fig. 3(b) gives $R \approx 1.07$. Using the value of $F_C=30$, F_{PC} is estimated to be $F_{\mathrm{PC}} \approx 0.6$, which qualitatively agrees with the values found in Refs. 2 and 11.

In conclusion, we have shown coupling of PbS quantum dots dissolved in PMMA to photonic crystal cavities at room temperature. The dot emission maps out the cavity resonances and is enhanced relative to the bulk emission by a maximal Purcell factor of 30. Using the emission spectra with and without cavity lines, we derive a photonic crystal lattice spontaneous emission rate modification of ≈0.6. To our knowledge, this is the first demonstration of coupling of colloidal quantum dots to photonic crystal cavities, and the first use of such dots as a broadband on-chip source for cavity characterization. Since such dots are available in a variety of emission wavelengths, this characterization technique can be applied to many different semiconductor devices. The deposition technique presented in this work is easy to use and allows many different types of emitters to be deposited and redeposited onto both passive and doped structures. Furthermore, electron-beam lithography can then be used to remove dot-doped PMMA from regions around the cavity, and the resulting emission will only come from the emitters in the cavity. The use of colloidal quantum dots for characterization of PC structures is similar to internal light source techniques,[12] but has a number of advantages: first, our method permits characterization of passive PC structures, where internal light sources are not available. Moreover, our technique allows deposition of sources on select areas on the chip, as well as redeposition and removal after characterization. Finally, our technique, combined with tuning of the quantum dot (QD) concentration in PMMA, can enable isolation of a single emitter inside the cavity, which would be beneficial for construction of single photon sources that are cheap and reusable, as opposed to those based on self-assembled QDs embedded in a PhC cavity.[2]

Financial support was provided by the MURI Center for photonic quantum information systems (ARO/ARDA Program DAAD19-03-1-0199), and the Stanford OTL Research Incentive. During this research I.F. was supported by a training grant from the National Institute of Health. Both I.F. and D.E. are supported by the NDSEG fellowship.

[1] J. Vučković and Y. Yamamoto, Appl. Phys. Lett. **82**, 3596 (2003).
[2] D. Englund, D. Fattal, E. Waks, G. Solomon, B. Zhang, T. Nakaoka, Y. Arakawa, Y. Yamamoto, and J. Vučković, Phys. Rev. Lett. **95**, 013904 (2005).
[3] E. Yablonovitch, J. Opt. Soc. Am. B **10**, 293 (1993).
[4] M. Soljačić and J. D. Joannopoulos, Nat. Mater. **3** (2004).
[5] B. Lounis and W. Moerner, Nature **407**, 491 (2000).
[6] A. Beveratos, R. Brouri, T. Gacoin, J. Poizat, and P. Grangier, Phys. Rev. A **64**, 061802 (2001).
[7] P. Michler, A. Imamoglu, M. Mason, P. Carson, G. F. Strouse, and S. K. Buratto, Nature **406**, 968 (2000).
[8] J. Vučković, M. Lončar, H. Mabuchi, and A. Scherer, Phys. Rev. E **65**, 016608 (2002).
[9] R. Ferrini, B. Lombardet, B. Wild, and R. Houdr, Appl. Phys. Lett. **82**, 1009 (2003).
[10] M. Scully and M. Zubairy, *Quantum Optics* (Cambridge University Press, Cambridge, 1997).
[11] R. Lee, R. Xu, and A. Yariv, J. Opt. Soc. Am. B **17**, 143842 (2000).
[12] D. Labilloy, H. Benisty, C. Weisbuch, T. Krauss, R. Houdré, and U. Oesterle, Appl. Phys. Lett. **71**, 738 (1997).